

# Probing the origin of giant radio halos through radio and $\gamma$ -ray data : the case of the Coma cluster

G. Brunetti,<sup>1\*</sup> P. Blasi,<sup>2†</sup> O. Reimer,<sup>3‡</sup> L. Rudnick,<sup>4§</sup> A. Bonafede,<sup>5¶</sup> S. Brown<sup>6||</sup>

<sup>1</sup> *INAF-IRA, Via Gobetti 101, I-40129 Bologna, Italy*

<sup>2</sup> *INAF-Osservatorio Astrofisico di Arcetri, Largo E. Fermi, 5, 50125 Firenze, Italy*

<sup>3</sup> *Institut für Astro- und Teilchenphysik, Leopold-Franzens-Universität Innsbruck, A-6020 Innsbruck, Austria*

<sup>4</sup> *Minnesota Inst. for Astrophysics, School of Physics & Astronomy, Univ. of Minnesota, 116 Church Street SE, Minneapolis, MN 55455, USA*

<sup>5</sup> *Jacobs University Bremen, Campus Ring 1, D-28759 Bremen, Germany*

<sup>6</sup> *CSIRO Astronomy & Space Science, P.O. Box 76, Epping NSW 1710, Australia*

Accepted —. Received —

## ABSTRACT

We combine for the first time all available information about the spectral shape and morphology of the radio halo of the Coma cluster with the recent  $\gamma$ -ray upper limits obtained by the Fermi-LAT and with the magnetic field strength derived from Faraday rotation measures. We explore the possibility that the radio emission is due to synchrotron emission of secondary electrons. First we investigate the case of pure secondary models that are merely based on the mechanism of continuous injection of secondary electrons via proton-proton collisions in the intra-cluster medium. We use the observed spatial distribution of the halo's radio brightness to constrain the amount of cosmic ray protons and their spatial distribution in the cluster that are required by the model. Under the canonical assumption that the spectrum of cosmic rays is a power-law in momentum and that the spectrum of secondaries is stationary, we find that the combination of the steep spectrum of cosmic ray protons necessary to explain the spectrum of the halo and the very broad spatial distribution (and large energy density) of cosmic rays result in a  $\gamma$ -ray emission in excess of present limits, unless the cluster magnetic field is relatively large. However this large magnetic field required to not violate present  $\gamma$ -ray limits appears inconsistent with that derived from recent Faraday rotation measures. Second we investigate more complex models in which the cosmic rays confined diffusively in the Coma cluster and their secondary electrons are all reaccelerated by MHD turbulence. We show that under these conditions it is possible to explain the radio spectrum and morphology of the radio halo and to predict  $\gamma$ -ray fluxes in agreement with the Fermi-LAT upper limits without tension with present constraints on the cluster magnetic field. Reacceleration of secondary particles also requires a very broad cosmic ray spatial profile, much flatter than that of the intracluster medium, at least provided that both the turbulent and magnetic field energy densities scale with that of the intracluster medium. However, this requirement can be easily alleviated if we assume that a small amount of (additional) seed primary electrons are reaccelerated in the cluster's external regions, or if we adopt flatter scalings of the turbulent and magnetic field energy densities with distance from the cluster center.

**Key words:** acceleration of particles - turbulence - radiation mechanisms: non-thermal - galaxies: clusters: general

## 1 INTRODUCTION

Galaxy clusters host several potential accelerators of cosmic ray (CR) electrons and protons, from ordinary galaxies to active galaxies (AGN) and cosmological shock waves, driven in the intracluster medium (ICM) during the process of hierarchical cluster formation (see Blasi et al. 2007 for a review).

The long lifetime of CR protons (or nuclei) in the ICM and the large geometrical size of the magnetized region of galaxy clusters make them efficient storage rooms for the hadronic component of CRs produced within their volume (Völk et al. 1996, Berezhinsky et al. 1997, Ensslin et al. 1997). The accumulation of CRs inside clusters over cosmological times leads to the assumption that an appreciable amount of energy may be stored in the ICM in the form of non-thermal particles. If this energy is sufficiently high, the flux of  $\gamma$  radiation induced by the production and decay of neutral pions may reach potentially detectable levels, thereby providing us with a powerful diagnostic tool of the CR energy content of clusters (Colafrancesco & Blasi 1998, Blasi & Colafrancesco 1999, Völk & Atoyan 1999, Miniati 2003, Pfrommer & Enßlin 2004, Wolfe et al. 2008).

So far only upper limits to the  $\gamma$ -ray emission from galaxy clusters have been obtained (Reimer et al. 2003; Perkins et al. 2006, Aharonian et al. 2009a,b; Aleksic et al. 2010; Ackermann et al. 2010) <sup>\*\*</sup>. These upper limits, together with several constraints from complementary approaches based on radio observations lead us to conclude that CR protons contribute less than a few percent of the energy of the ICM, at least in the central Mpc-size region (Reimer et al. 2004, Brunetti et al. 2007, 2008, Brown et al. 2011, Aleksic et al. 2011).

CR electrons are very well traced in the ICM through their radio emission which appears in the form of diffuse (Mpc scale) synchrotron *giant radio halos* from the cluster X-ray emitting regions, and *relics*, typically in the clusters' peripheral regions (see Ferrari et al. 2008, Venturi 2011, for recent reviews on observations).

Giant radio halos are the most spectacular and best studied non-thermal large scale phenomena in the universe. They appear in about 1/3 of the most massive galaxy clusters (e.g. Giovannini et al. 1999, Kempner & Sarazin 2001, Cassano et al. 2008), in a rather clear connection with dynamically disturbed systems, while “off-state” clusters (those with no evidence of diffuse emission) are generally more relaxed (Cassano et al. 2010a and references therein). The connection between cluster mergers and radio halos suggests that such emission traces the hierarchical cluster assembly and probes the dissipation of gravitational energy during the dark matter-driven mergers that lead to the formation of clusters. The physical mechanisms responsible for the generation and evolution of radio halos are still a matter of debate, but two main lines of thought have been developed throughout the years.

One is based on the idea that seed electrons may be re-accelerated by turbulence produced during merger events (Brunetti et al. 2001, Petrosian 2001). In this class of models the  $\gamma$ -ray emission is predicted to be rather low, though it may be substantial under the hypothesis that the electron seeds are secondaries produced in inelastic collisions of a subdominant hadronic CR component in the ICM (Brunetti & Blasi 2005; Brunetti & Lazarian 2011).

The second line of thought is based on the idea of clusters as storage rooms of CR protons: the radio halos may be generated as a result of synchrotron emission of secondary electrons and positrons from pp collisions (Dennison 1980, Blasi & Colafrancesco 1999, Pfrommer & Enßlin 2004). On one hand this idea serves as a solution to the problem of the large spatial dimensions of the radio emitting region, larger than the typical loss length of electrons: secondary electrons and positrons are produced *in situ* in inelastic CR collisions and radiation is produced near the production region. On the other hand, secondary models do not explain in a *natural* way the observed association between cluster mergers and giant radio halos, in that CRs accumulate inside the ICM on cosmological time scales and not in direct connection with acceleration events such as those associated with mergers <sup>††</sup>. One proposal is that during merger events the cluster magnetic field becomes larger than in the quiescent state, thereby turning the halo on (Kushnir et al. 2009, Keshet & Loeb 2010), although studies based on Rotation Measures of clusters' and background radio sources disfavour this scenario (see Bonafede et al. 2011a and ref. therein). In fact, some pieces of observations put tension on a *pure* hadronic origin of radio halos. These include the steepening in the spectrum (or the very steep spectrum) of several halos (Schlickeiser et al. 1987, Thierbach et al. 2003, Reimer et al. 2004, Brunetti et al. 2008, Dallacasa et al. 2009, Giovannini et al. 2009, Macario et al. 2010, van Veeren et al. 2011) and the very large spatial extent of several halos (or their flat radio-brightness distribution) (Brunetti 2004, Murgia et al. 2009, Donnert et al. 2010a, Brown & Rudnick 2011); in all cases observations would imply that the energy budget of CR protons is uncomfortably large,

\* E-mail: brunetti@ira.inaf.it

† E-mail: blasi@arcetri.astro.it

‡ E-mail: Olaf.Reimer@uibk.ac.at

§ E-mail: larry@astro.umn.edu

¶ E-mail: a.bonafede@jacobs-university.de

|| Bolton Fellow, E-mail: Shea.Brown@csiro.au

\*\* See however Han et al. 2011 for Virgo

†† see however Ensslin et al. 2011, where diffusion/transport of CRs is studied under peculiar conditions

at least assuming that clusters are magnetised at  $\sim \mu\text{G}$  level, consistent with the results of RM (see Bonafede et al. 2010 and references therein).

The most distinct prediction of models of radio halos that are based on secondary particles is the production of  $\gamma$ -rays (e.g., Blasi & Colafrancesco 1999, Sarazin 2004, Pfrommer & Enßlin 2004, Brunetti 2009, Brunetti & Lazarian 2011, Enßlin et al. 2011). Nowadays there is agreement on the fact that the abundance of secondaries required to fit the spectrum of (at least some) radio halos should produce  $\gamma$ -ray emission detectable with the sensitivity of the Fermi-LAT, assuming low/medium level of cluster magnetic field (eg. Marchegiani et al 2007, Pfrommer 2008, Brunetti 2009, Jeltama & Profumo 2011). Thus the combination of the available information on the spectrum and morphology of radio halos in conjunction with the limits on their  $\gamma$ -ray emission provides a powerful tool to gain insights into the origin of the halo emission.

Following this pathway, in this paper we concentrate on the case of the Coma cluster, which represents a prototypical example of giant radio halos, with a wealth of data available on its spectrum and morphology. The incoming upper limits on the Coma  $\gamma$ -ray emission with the Fermi-LAT telescope are invaluable in imposing stringent limits on the amount of cosmic rays that can be stored in the intracluster medium and serve as sources of secondary electrons and positrons. In particular in this paper we combine for the first time all available information about the spectral shape and morphology of the radio halo of the Coma cluster with the recent  $\gamma$ -ray upper limits and magnetic field strengths derived from Faraday rotation measures. We show that the requirement of reproducing the properties of the Coma radio halo in the context of a pure secondary electron model leads to a large CR energetics and fluxes of  $\gamma$ -rays which results in a tension with the existing upper limits from the Fermi-LAT (Ackermann et al. 2010). This situation is readily alleviated in the case of a large cluster magnetic field, however the magnetic fields required by the model are appreciably larger than those inferred from recent Faraday rotation measures.

This tension disappears when including the effect of turbulent reacceleration in combination with the process of injection of secondary particles. We adopt a physically motivated picture in which secondary products of cosmic ray interactions are reaccelerated by MHD turbulence during clusters mergers. In this sense we value the physical insight behind the concept of cosmic ray confinement and the production of secondary electrons, but we do not assume that these particles are “directly” responsible for the formation of the radio halo. We find that even reacceleration models of this type require a broad spatial distribution of the parent cosmic rays, but the expected  $\gamma$ -ray fluxes are well consistent with the Fermi-LAT upper limits.

The paper is organized as follows: we discuss the hadronic model of radio emission in §2 and the reacceleration model in §3. A critical discussion of our results is provided in §4. A  $\Lambda\text{CDM}$  cosmology ( $H_o = 70 \text{ km s}^{-1} \text{ Mpc}^{-1}$ ,  $\Omega_m = 0.3$ ,  $\Omega_\Lambda = 0.7$ ) is adopted throughout the paper.

## 2 PURE HADRONIC MODELS

### 2.1 Formalism : radio and $\gamma$ -ray emission

The decay chain responsible for the injection of secondary particles in the ICM due to p-p collisions is (e.g., Blasi & Colafrancesco 1999):

$$\begin{aligned} p + p &\rightarrow \pi^0 + \pi^+ + \pi^- + \text{anything} \\ \pi^0 &\rightarrow \gamma\gamma \\ \pi^\pm &\rightarrow \mu^\pm + \nu_\mu, \quad \mu^\pm \rightarrow e^\pm \nu_\mu \nu_e. \end{aligned}$$

The initial inelastic scattering reaction occurs at threshold, namely it requires protons with kinetic energy larger than  $T_p \approx 300 \text{ MeV}$ . The injection rate of pions is

$$Q_{\pi^{\pm,0}}^{\pm,0}(E_{\pi^{\pm,0}}, t) = n_{th} c \int_{p_*} dp N_p(p, t) \beta_p \frac{F_\pi(E_\pi, E_p) \sigma^{\pm,0}(p)}{\sqrt{1 + (m_p c/p)^2}}, \quad (1)$$

where  $n_{th}$  is the number density of thermal (target) protons,  $N_p$  is the spectrum of cosmic ray protons, and  $F_\pi$  is the spectrum of pions from the collision between a CR proton of energy  $E_p$  and thermal protons (taken from Brunetti & Blasi 2005). The inclusive cross-section,  $\sigma(p)$ , is taken from the fitting formulae of Dermer (1986b), which allows us to describe separately the rates of generation of  $\pi^-$ ,  $\pi^+$ , and  $\pi^0$ , and  $p_* = \max\{p_{tr}, p_\pi\}$ , where  $p_{tr}$  is the threshold momentum of protons for pion production (different for charged and neutral pions).

Charged pions decay into muons and then secondary pairs (electrons and positrons). If secondaries are not accelerated by other mechanisms and the physical conditions in the ICM do not change on time-scales shorter than the electrons' radiative

time  $\ddagger\ddagger$ , their spectrum approaches a stationary distribution because of the competition between injection and energy losses (e.g., Dolag & Ensslin 2000), and one can write:

$$N_e^\pm(p) = \frac{1}{\left| \left( \frac{dp}{dt} \right)_{\text{loss}} \right|} \int_p^{p_{\text{max}}} Q_e^\pm(p) dp, \quad (2)$$

where  $Q_e^\pm$  is the injection rate of secondaries (Blasi & Colafrancesco 1999; Moskalenko & Strong 1998), and radiative losses, which are dominant for  $\gamma > 10^3$  electrons in the ICM, can be written as (Sarazin 1999):

$$\left| \left( \frac{dp}{dt} \right)_{\text{loss}} \right| \simeq 3.3 \times 10^{-32} \left( \frac{p/m_e c}{300} \right)^2 \left[ \left( \frac{B_{\mu G}}{3.2} \right)^2 + (1+z)^4 \right]. \quad (3)$$

Assuming a power law (momentum) distribution of CR protons,  $N_p(p) = K_p p^{-s}$ , the spectrum of secondaries at high energies,  $\gamma > 10^3$ , is  $N_e(p) \propto p^{-(s+1)} \mathcal{F}(p)$ , where  $\mathcal{F}$  accounts for the log-scaling of the p-p cross-section at high energies and causes the spectral shape to be slightly flatter than  $p^{-(s+1)}$  (Brunetti & Blasi 2005). The synchrotron spectrum from secondary  $e^\pm$  is (Rybicky & Lightman 1979):

$$J_{syn}(\nu) = \sqrt{3} \frac{e^3}{m_e c^2} B \int_0^{\pi/2} d\theta \sin^2 \theta \int dp N_e(p) F\left(\frac{\nu}{\nu_c}\right) \simeq C_{syn}(\alpha, T) X n_{th}^2 \frac{B^{1+\alpha}}{B^2 + B_{cmb}^2} \nu^{-\alpha}, \quad (4)$$

where  $C_{syn}$  is a constant,  $X = \epsilon_{CR}/\epsilon_{ICM}$  is the ratio of the energy densities of CR protons to thermal protons,  $F$  is the synchrotron kernel,  $\nu_c$  is the critical frequency, and  $\alpha \simeq s/2 - \Delta$  is the synchrotron spectral index, where  $\Delta \sim 0.1$  (in the conditions of interest for our paper) is due to the log-scaling of the cross-section.

The spectrum of  $\gamma$ -rays produced by secondary particles is dominated by the decay of the secondary  $\pi^0$  (Dermer 1986ab; Blasi & Colafrancesco 1999, Blasi 2001) :

$$Q_\gamma(E_\gamma) = 2 \int_{E_{min}}^{E_p^{max}} \frac{Q_{\pi^0}(E_{\pi^0})}{\sqrt{E_\pi^2 - m_\pi^2 c^4}} dE_\pi, \quad (5)$$

where  $E_{min} = E_\gamma + m_\pi^2 c^4 / (4E_\gamma)$ . Under the same assumptions as Eq.4, the  $\gamma$ -ray emissivity for  $h\nu_\gamma > \text{GeV}$  is:

$$J_\gamma(\nu) \simeq C_\gamma(s, T) X n_{th}^2 \nu^{-\tilde{s}}, \quad (6)$$

where  $C_\gamma$  is a constant and  $\tilde{s} \sim s - 1$ . This gives a minimum estimate of the cluster  $\gamma$ -ray emission since IC and non-thermal bremsstrahlung emission from secondary and primary electrons provide additional contributions (e.g. Sarazin 1999, Blasi 2001, Miniati 2003).

## 2.2 Testing hadronic models for radio halos

The ratio of the synchrotron and  $\gamma$ -ray cluster luminosities depends on the magnetic field in the emitting volume (from Eqs. 4 and 6). By considering reasonable assumptions on the magnetic field in galaxy clusters several authors suggested that observations by the Fermi-LAT may have the chance to detect  $\gamma$ -rays from nearby clusters hosting radio halos (Pfrommer & Enßlin 2004, Marchegiani et al. 2007, Pfrommer 2008, Wolfe et al. 2008, Brunetti 2009).

More recently, Jeltema & Profumo (2011) analysed the impact of limits on the  $\gamma$ -ray emission from clusters of galaxies (Ackermann et al. 2010) on hadronic models for the origin of cluster radio halos, deriving lower limits on the average cluster magnetic field. In some cases of nearby radio halos they find that these lower limits are close to (or larger than) the magnetic field values inferred from Faraday rotation measures, thereby placing tension on the hadronic origin of radio halos. In their analysis Jeltema & Profumo used the total radio luminosity and the  $\gamma$ -ray upper limits.

Here we discuss the possibility that even more stringent limits may be obtained by using the information about the morphology of the radio emission *in addition* to the total luminosity. Giant radio halos have flat brightness distributions, in several cases flatter than the thermal X-ray emission of the hosting clusters (e.g. Govoni et al. 2001, Feretti et al. 2001, Brown & Rudnick 2011), implying that most of the synchrotron emission is produced in the external regions where the magnetic field is smaller. Thus, we anticipate a larger energy budget of CR protons compared with that needed to explain only the total luminosity of radio halos (Brunetti 2004, Donnert et al. 2010a,b). The consequence is also a larger  $\gamma$ -ray luminosity from the hosting clusters (Donnert et al. 2010a).

Given these premises, in Sect. 2.3 we attempt to analyse the impact of the Fermi-LAT upper limits from the Coma cluster. We summarize our assumptions as follows:

$\ddagger\ddagger$  see Keshet (2010) for a discussion on effects due to variations of magnetic fields on shorter time-scales

- i)* The spectrum of cosmic ray protons is assumed to be a power law in momentum, as results from most acceleration mechanisms,  $N(p) = K_p p^{-s}$ ;
- ii)* The spatial distribution of the gas in the ICM is taken to follow the *observed*  $\beta$ -model that is parameterised according to thermal density at the cluster center,  $n_{th}(0)$ , the core radius,  $r_c$  kpc, and  $\beta$ ;
- iii)* The spatial distribution of the energy density of CR protons in the cluster volume is parametrized as  $\epsilon_{CR} \propto \epsilon_{ICM}^{1+f}$ ;
- iv)* The magnetic field strength is assumed to scale with location  $r$  in the ICM according with  $B(r) = B_0 [\epsilon_{ICM}(r)/\epsilon_{ICM}(0)]^\eta$ ,  $\eta = 0.5$  implies that the magnetic field energy density scales with the thermal one.

Within these assumptions the synchrotron emissivity from secondary particles (from Eq. 4) is:

$$J_{syn}(\nu) \propto n_{th}^{2+f} T^{1+f} \frac{(n_{th} T)^{\eta(1+\alpha)}}{C_B^2 (n_{th} T)^{2\eta} + B_{cmb}^2}, \quad (7)$$

which implies a synchrotron brightness (assuming  $T$  constant on  $\sim 1$  Mpc scale to derive simple scalings)  $I_{syn} \propto (1 + x^2)^{-3\tilde{\beta}+1/2}$ , where  $x$  is the projected distance in units of the core radius,  $C_B$  is a constant ( $B = C_B (n_{th} T)^\eta$ ), and  $\tilde{\beta} = \beta(2 + f + (\alpha - 1)\eta)/2$  and  $\hat{\beta} = \beta(2 + f + (\alpha + 1)\eta)/2$  in the case  $B^2(x) \gg B_{cmb}^2$  and  $B^2(x) \ll B_{cmb}^2$ , respectively.

For a given model of magnetic field distribution,  $(B_0, \eta)$ , the three key parameters characterizing the radio emissivity and then the predictions for the  $\gamma$ -ray emission are thus :

1.  $s$ : the logarithmic slope of the momentum distribution of CR protons, determined from measurements of the radio spectral index  $\alpha$ . Typically  $s \sim 2.3 - 3$  (for some halos with ultra-steep spectrum  $s > 3$ );
2.  $f$ : the non-linear scaling of the energy density of CR protons with the thermal ICM energy density, derived from the shape of the synchrotron brightness profile of the radio halo;
3.  $K_p$ : the normalization of the momentum distribution of CR protons, determined from the radio luminosity of the halo.

The outcome of this procedure is the expected  $\gamma$ -ray emission from  $\pi^0$ -decays.

### 2.3 Application to the Coma radio halo

The radio halo in the Coma cluster (Coma C) is the prototypical cluster radio halo (e.g., Willson 1970, Giovannini et al. 1993). It is unique in that its spectrum is measured over a wide frequency range (Fig. 1, left panel). The spectrum shows a significant steepening at high frequencies: a power-law that fits the data at lower frequencies overestimates the flux measured at 2.7 and 5 GHz by a factor 2 and 4 respectively (Schlickeiser et al. 1987, Thierbach et al. 2003). In secondary electron models the electron spectrum extends in principle to very high energies, therefore no intrinsic cutoff is expected in the radio spectrum. The observed spectral steepening is therefore inconsistent with secondary electron models (Schlickeiser et al. 1987, Brunetti et al. 2001, Petrosian 2001, Blasi 2001, Reimer et al 2004) unless unnatural assumptions are made on the CR proton spectrum. Enßlin (2002) suggested that the steepening at higher frequencies may be due to the thermal SZ-decrement (suppression of the CMB spectrum seen in the direction of the cluster from the up-scattering of the CMB photons due to Compton scattering with the thermal electrons in the ICM). Calculations carried out by Brunetti (2004) and Reimer et al. (2004) showed that this is not the case when the SZ estimate is limited to the region covered by the halo emission. More recent investigations, based on numerical simulations confirm these calculations showing that the effect of the SZ decrement on the Coma spectrum at 2.7 and 5 GHz is not sufficient to explain the observed spectral break (Donnert et al. 2010a).

The halo shows a fairly regular morphology on a scale  $\sim 1.5$  Mpc with a radio brightness profile  $I_{syn}(r)$  that is flatter than the X-ray (thermal) profile  $I_X$  (Govoni et al. 2001, Brown & Rudnick 2011). The global point-to-point power-law correlation between the 0.3 GHz radio brightness and the X-ray brightness,  $I_{syn} \propto I_X^{0.64}$ , implies that most of the radio emission is produced outside the cluster core,  $r_c \sim 270$  kpc. The brightness profile of radio halos is an important observable quantity that provides constraints on the spatial distribution of CRs and magnetic fields in the cluster (Brunetti 2004, Pfrommert & Enßlin 2004, Colafrancesco et al. 2005, Donnert et al 2010a). We measure the radial profile of the Coma halo using the new WSRT observations at 350 MHz by Brown & Rudnick (2011) and obtain unprecedented constraints on the brightness distribution of the halo up to 3-3.5  $r_c$  distance from the cluster center. The radial (azimuthally averaged) brightness profile is shown in Fig. 1 (right panel) and is compared with other profiles available in the literature, Govoni et al. (2001) at 350 MHz, and Deiss et al (1997) at 1.4 GHz. The new brightness profile provides constraints that are significantly better than those from previous observations and, most important, they extend to larger spatial scales. The brightness profile is much flatter than the one found by Deiss et al., that has been widely adopted in the literature (Pfrommert & Enßlin 2004, Colafrancesco et al 2005, Donnert et al 2010a), implying that the amount of energy in the form of CRs and magnetic field at distances  $\sim 2 - 3.5 r_c$  from the cluster center is much larger than previously thought.

The inset in the right panel of Fig. 1 shows the cumulative flux profile of the Coma halo (based on Brown & Rudnick 2011). Assuming a central value of the magnetic field  $B_0 \sim 5\mu\text{G}$  and  $\eta = 0.5$  (Bonafede et al. 2010), about 70-80% of the observed radio luminosity is produced in regions where  $B^2 \ll B_{cmb}^2$ , while synchrotron dominance is expected only inside the cluster's

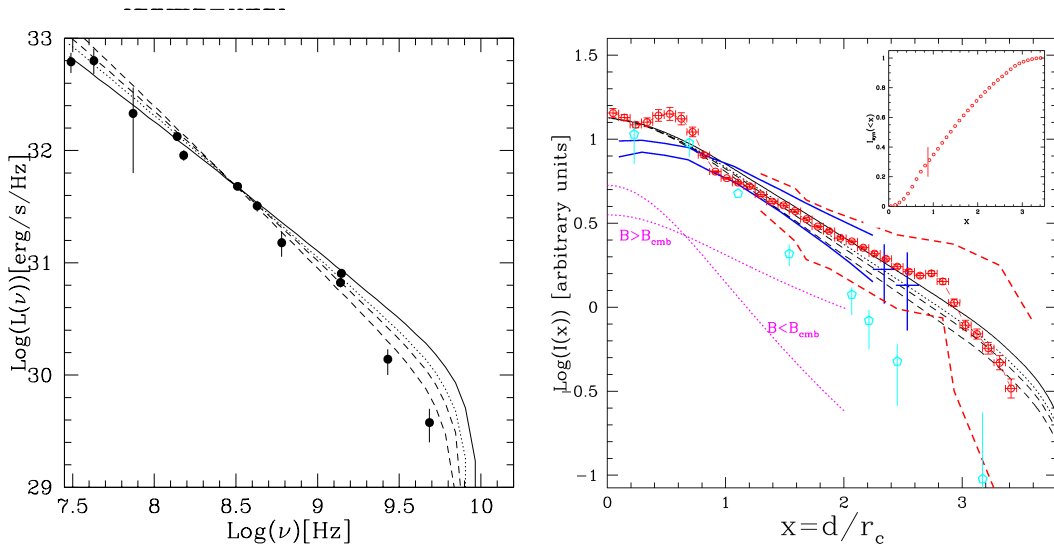


**Figure 1.** **Left:** Spectrum of the Coma halo from hadronic models assuming a slope  $s = 2.6$  (solid), 2.85 (dotted), 3, 3.25 (dashed) (compilation of data points taken from Pizzo 2010). Models are normalised at 350 MHz. The steepening at higher frequencies in the models is due to the thermal SZ-decrement (see text). **Right:** The measured brightness (azimuthal averaged) profile of the Coma halo (in arbitrary units) at 350 MHz, using observations in Brown & Rudnick (2011), is shown as a function of distance in units of core radius,  $r_c = 270$  kpc (red points). Red dashed lines mark the upper and lower envelope of the measured profile taken along different directions (from Brown & Rudnick). The new measurements are compared with previous data at 350 MHz from Govoni et al.(2001) (solid, blue and crosses) and with data at 1.4 GHz from Deiss et al.(1997) (cyan points). The brightness profile from hadronic models is shown assuming  $B_0 \sim 5\mu\text{G}$ ,  $\eta = 0.5$  and  $f = -1.6$  for  $s = 2.6$  (same line-type as in the left panel). The inset shows the cumulative flux profile calculated using the Brown & Rudnick azimuthal averaged profile, the vertical line shows the transition between the regime of synchrotron-dominance (smaller distances) and IC-dominance (larger distances from cluster center). Finally the (magenta) dotted-lines show the expected shape of the brightness profile assuming hadronic models with  $f = -1.0$ , with synchrotron-dominance and IC-dominance (scalings derived in the paragraph below Eq.7); for display purposes the magenta profiles are not normalised to the data.

core. In the right panel of Fig. 1 the (magenta) dotted-lines show the case of a hadronic model of the radio halo, with the shape of the expected synchrotron spectrum chosen to match the observed synchrotron spectral index,  $\alpha \sim 1.3$  (Deiss et al. 1997),  $\beta = 0.75$ , and a flat spatial distribution of CR protons ( $f = -1$ ). In the relevant case  $B^2 \ll B_{cmb}^2$ , the expected brightness is steeper than the observed one, implying that the energy density of CRs must increase with distance (at least up to about  $r \sim 2.5 - 3r_c$ ) in order to fit the observed radio profile. This has consequences on the total energy budget of CRs in the external regions of the cluster and on the expected  $\gamma$ -ray emission.

We adopt a general modeling of the non-thermal CR proton distribution in the Coma radio halo,  $\epsilon_{CR} \propto \epsilon_{ICM}^{1+f}$  for  $r \leq R_H$  ( $R_H \sim 3r_c$  being the halo radius) and  $\epsilon_{CR} \propto \epsilon_{ICM}$  for  $r > R_H$ . This provides us with a conservative approach that minimizes the energy budget of CR protons in the very external regions ( $r > 3 - 3.5r_c$ ), where present data do not provide reliable constraints. Under these conservative assumptions the  $\gamma$ -ray brightness profile becomes steeper at projected distance  $d \geq R_H$  where the brightness becomes proportional to that of the thermal X-ray emission; from Eq. 6 it is  $I_\gamma(d)d^2 \propto d^{-6\beta+3}$ , implying that the majority of the  $\gamma$ -rays are produced within  $\sim R_H$ .

The observed radio luminosity at 350 MHz and the brightness profile allow us to constrain  $K_p$  (see Sect. 2) and consequently to estimate the  $\gamma$ -ray luminosity for a given model of the cluster magnetic field. In order to break the degeneracy with the magnetic field properties, as a *reference point* we start by assuming the magnetic field strength and its spatial distribution as derived from the analysis of RM (Bonafede et al. 2010). Bonafede et al. analyzed polarization data for seven radio sources in the Coma cluster field observed with the VLA at 3.6, 6 and 20 cm. They derived Faraday rotation measures with kpc scale resolution and compared observations with simulations of random three-dimensional magnetic field models where the magnetic field was scaled with the thermal cluster density in the form  $B(r) \propto B_0 n_{th}(r)^\eta$ . They derive constraints for the magnetic field strength and profile ( $B_0, \eta$ ) with best values  $B_0 = 4.7\mu\text{G}$  and  $\eta = 0.5$ , respectively;  $\eta \sim 0.5$  is also consistent with results from recent numerical MHD simulations of a variety of clusters (Bonafede et al. 2011b).

The  $\gamma$ -ray emission from  $\pi^0$  decay as calculated for the same choice of parameters as in Fig. 1 is shown in Fig. 2 (left panel) together with the Fermi-LAT upper limits from the first 18 month of observations (Ackermann et al. 2010). We are using the Ackermann et al. limits derived by choosing a Gaussian (with 68% surface intensity containment radius = 0.4 and 0.6 deg) spatial distributions of  $\gamma$ -rays; this is consistent with the spatial distribution expected from the model we adopted here (Fig. 2, right panel). The comparison between the predictions of the model and the existing upper limits is therefore to be considered fair. In Fig. 2 (left panel, dashed) we also show the level of the upper limit assuming no detection after 3

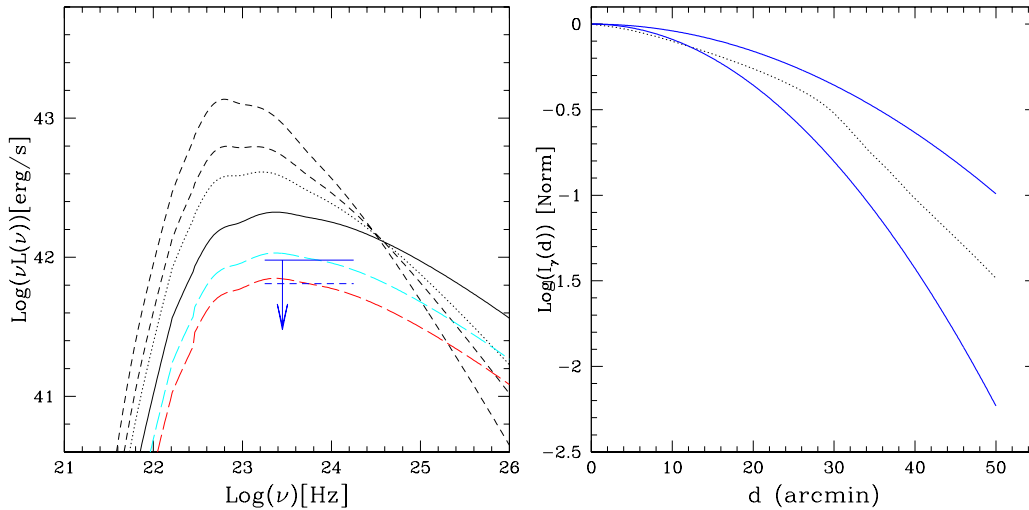


**Figure 2.** **Left:**  $\gamma$ -ray spectrum due to  $\pi^0$ -decay from hadronic models in Fig. 1. The blue solid and dashed arrows mark the Ackermann et al. 2010 1–10 GeV limit and that extrapolated by assuming no detection after 3 years of FERMI observations, respectively. To highlight the effect due to constraints from the radio brightness profile on the predicted  $\gamma$ -ray emission we also show expectations for  $\delta = 2.6$  assuming the old brightness profile from Deiss et al. (1997) (cyan, long-dashed line) and assuming  $f = 0$  (red, long-dashed line). **Right:** The  $\gamma$ -ray brightness profile from hadronic models in Fig. 1 compared with the Gaussians with 68% surface intensity containment radius = 0.4 and 0.6 deg that are chosen in Ackermann et al. to derive the value of the Fermi-LAT upper limit used in our paper.

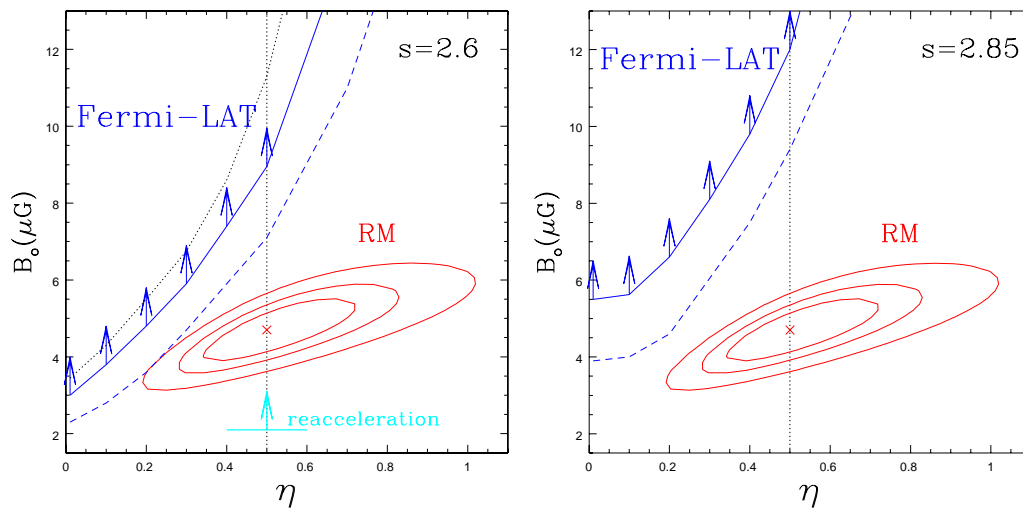


**Figure 3.** **Left:** A comparison between the allowed region ( $B_0, \eta$ ) from the analysis of RM by Bonafede et al. 2010 (contours are reported at 1, 2, 3  $\sigma$ ) and that allowed, assuming a hadronic origin of the radio halo with a slope of CR protons  $s = 2.6$ , by the  $2\text{-}\sigma$  upper limit from Ackermann et al. (dashed), assuming no detection from 3 years of Fermi-LAT observations (extrapolated from Ackermann, solid line), and using the  $2\text{-}\sigma$  upper limit from Han et al. (2012) (dotted). The vertical dotted line marks the relevant case  $\eta = 0.5$ , in this case a lower limit to  $B_0$  obtained by assuming a reacceleration model (Sect.3) is reported (cyan). **Right:** The same as in Left panel but assuming  $s = 2.85$ ; for simplicity here we do not report limits obtained by using Han et al. (2012).

years of observations;<sup>§§</sup> that is obtained by simply scaling the Ackermann’s upper limit according to the square root of the exposure time. For sake of clarity, in Fig.2 we also show the expected  $\gamma$ -rays in the case we assume a constant ratio of the

<sup>§§</sup> Ando & Nagai (2011) and Han et al. (2012) presented a analysis of 3 years of Fermi-LAT observations of nearby galaxy clusters. They both report a  $2\sigma$  upper limit for the Coma cluster.

CR protons and thermal energy densities in the cluster ( $f = 0$ , red long-dashed line), i.e. without considering the constraints from the radio brightness distribution of the Coma halo (see also Sect. 4 and Fig. 4).

Our results show that a pure hadronic origin of the halo is inconsistent with the Fermi-LAT upper limit, if the magnetic field properties are parametrized to satisfy the best fit obtained by Bonafede et al. (2010). Remarkably, the radio spectrum plotted in the left panel of Fig. 1 shows that the spectrum of the halo is best fitted assuming steeper CR spectra. This happens because the effect of the negative flux from the thermal SZ-decrement becomes more relevant when the radio flux of the halo at high frequencies is smaller (see also Pfrommer & Enßlin 2004). However, steeper CR spectra produce more  $\gamma$ -rays at low energy and a hadronic origin of the halo is readily ruled out by using the Fermi-LAT upper limits.

The choice of the value of  $\eta$  has a significant impact on the expected  $\gamma$ -ray emission from the cluster because it determines the amount of CR protons that must be assumed at different distances from the cluster center to match the observed synchrotron profile. There are some observational and theoretical arguments that suggest that the ratio of turbulent and thermal pressure in clusters may increase in the cluster external regions (e.g. Vazza et al 2009, Iapichino et al 2011, Churazov et al 2012) which may eventually imply that the ratio of magnetic field and thermal energy densities could increase with cluster distance (assuming that magnetic field and turbulent energy correlate). For this reason we carry out more general calculations assuming  $\eta$  in the range 0–1. This is shown in Fig. 3 using present (Ackermann et al. 2010) Fermi-LAT upper limits (dashed line), and assuming no detection of  $\gamma$ -rays from the Coma cluster after 3 years of observations (solid line, obtained by simply scaling the Ackermann et al. limit according to the square root of the exposure time); lower limits obtained by using very recent Fermi-LAT upper limits by Ando & Nagai (2011) and Han et al. (2012) are also shown for the sake of completeness (dotted line). For large values of  $\eta$  ( $\eta > 0.5$ ) the constraints are more stringent and only implausibly large values of  $B_0$  are allowed. On the other hand for small values of  $\eta$  fewer CR protons are required to match the radio luminosity and the brightness profile of the halo, leading to less stringent constraints on the magnetic field strength. In particular the minimum value of  $B_0$  increases with  $\eta$ , from about  $B_0 \geq 3\mu\text{G}$  for  $\eta = 0$  ( $B_0 \geq 5.5\mu\text{G}$  for  $\delta = 2.85$ ) to  $B_0 \geq 8.5\mu\text{G}$  for  $\eta = 0.5$  ( $B_0 \geq 11\mu\text{G}$  for  $\delta = 2.85$ ).

In Fig. 3 we also show constraints on the values of  $B_0 - \eta$  as obtained by Bonafede et al. We find disagreement between the region constrained from the analysis of RM and that allowed by the lower limits on  $B_0$  as obtained from the Fermi-LAT limits. In the relevant case  $\epsilon_B \propto \epsilon_{ICM}$  ( $\eta = 0.5$ ), we find that the minimum magnetic field energy density allowed by Fermi-LAT limits is 5-10 times larger than that of the *reference* magnetic field energy density, estimated from the analysis of RM, while for  $\eta = 0.2$  (still consistent with RM within  $3\sigma$ ) the discrepancy is reduced to a factor  $\sim 2$ ; the discrepancy becomes severe for  $\eta > 0.5$ . In general it is worth stressing here that our constraints using upper limits from 3 years of Fermi-LAT observations select high magnetic fields, in which case even a moderate improvement of the  $\gamma$ -ray limits implies a substantial increase of the minimum value of the magnetic field that is allowed (for example, in the case  $\eta \sim 0$  and  $B_0 > B_{cmb}$  it is  $B_{\min} \propto J_{\gamma(ul)}^{1/(1-\alpha)\sim -3}$ , from Eqs.5–6). Consequently deeper upper limits from Fermi-LAT in the next years, or even a detection of the Coma cluster at a level 2-3 times below Ackermann et al. limits will considerably increase the difficulties in the context of a *pure* hadronic model for the radio halo.

Using the Ackermann et al. upper limits, in the relevant case  $\eta = 0.5$  Jeltema & Profumo (2011) infer a value of the minimum magnetic field in the cluster center,  $B_0 > 3.9\mu\text{G}$ , a result that is still consistent with the values constrained from RM. The difference between our work and Jeltema & Profumo (2011) essentially stems from the adopted spatial distribution of CRs in the cluster. Jeltema & Profumo (2011) assumed  $\epsilon_{CRp} \propto \epsilon_{ICM}$  while in our calculations we used the spatial distribution of CR protons needed to reproduce the observed synchrotron brightness profile of the radio halo. In order to highlight this point, in Fig. 4 we show the ratio of the  $\gamma$ -ray luminosity that is obtained assuming a scaling  $\epsilon_{CRp} \propto \epsilon_{ICM}^{1+f}$  and that assuming a linear scaling ( $f = 0$ ) between the energy densities of CRs and ICM. In Fig. 4 we also report the constraints on  $f$  derived from the synchrotron brightness profile of the halo and the limits implied by the Fermi-LAT upper limits after 18 months of observations (Ackermann et al. 2010) and by assuming no detection of the Coma cluster after  $\sim 3$  years of observations. We confirm that assuming  $f = 0$  (as in Jeltema & Profumo) the value of the central magnetic field constrained from the Ackermann et al.  $\gamma$ -ray upper limits is still consistent with the value inferred from RM ( $B_0 = 4.7\mu\text{G}$ , with  $\eta = 0.5$ , Bonafede et al. 2010), however in this case the synchrotron brightness profile of the halo is predicted to be considerably steeper, inconsistent with the observed one (Fig. 4, inset).

Finally we stress here that the discussion above considers a *reference* value for the magnetic field in the Coma cluster based on an analysis of RMs. These results are obtained by assuming that the RM originates entirely in the ICM (Bonafede et al. 2010). If a contribution local to the radio galaxies is present, as found in other cases (e.g. Rudnick & Blundell 2003, Guidetti et al. 2011), the values of the magnetic field in the ICM, as inferred from the observed RM, would be biased to higher values (see Rudnick & Blundell 2003) and the *reference* value should be considered as an upper limit to the actual cluster field. This case would make our conclusions even stronger.

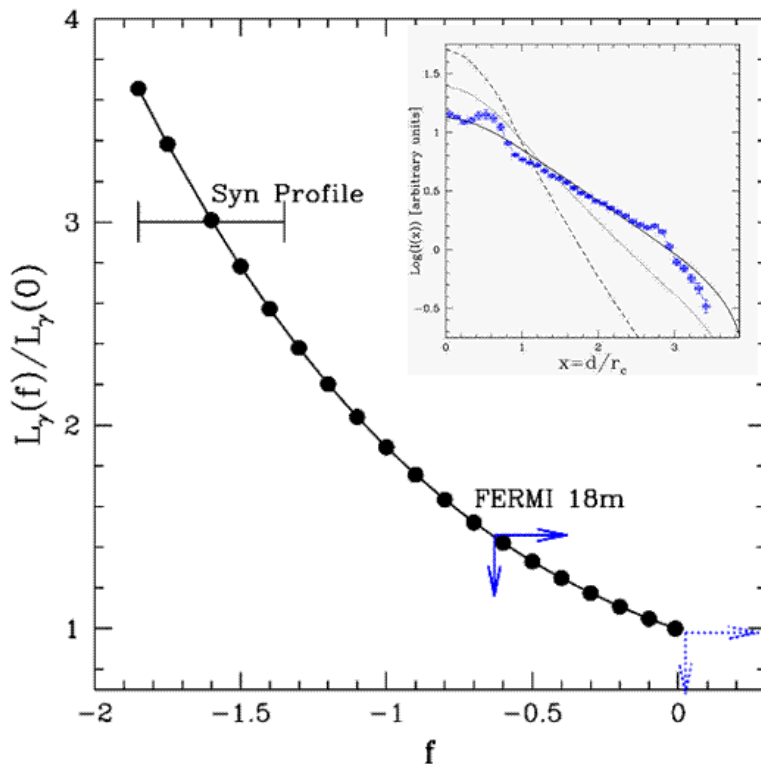


**Figure 4.** The  $\gamma$ -ray luminosity of the Coma cluster assuming hadronic models for the radio halo (assuming  $B_0 = 4.7\mu\text{G}$ ,  $\eta = 0.5$  and  $s = 2.6$ ) is shown as a function of  $f$  and normalised to that expected for  $f = 0$  (namely assuming a scaling  $\epsilon_{CR} \propto \epsilon_{ICM}$  as in Jeltema & Profumo 2011). The inset shows the comparison between the observed brightness profile of the Coma halo and expectations based on hadronic models with  $f = -1.6, -1.0, 0$  (from flatter to steeper). The horizontal error-bar gives the values of  $f$  as constrained ( $3\text{-}\sigma$ ) from the observed brightness profile (we consider the slope of the profile in the distance range  $1\text{--}2.5 r_c$ ). Blue arrows give the Fermi-LAT upper limits (solid= Ackermann et al.(2010), dotted= extrapolation of Ackermann’s limit at 3 years observation) and their implications for the parameter  $f$ .

### 3 TURBULENT ACCELERATION OF SECONDARY ELECTRONS AND POSITRONS

Models based on turbulent reacceleration of seed electrons (Schlickeiser et al. 1987, Brunetti et al. 2001, Petrosian 2001, Fujita et al. 2003, Cassano & Brunetti 2005) rely upon the observed low efficiency of particle acceleration in the ICM, as suggested for instance by the  $\geq 1$  GHz cutoff in the radio spectrum of Coma (Schlickeiser et al. 1987, Thierbach et al. 2003), and the fact that radio halos are not common and are correlated with clusters’ dynamics (see discussion in Brunetti et al. 2009). More recently, (indirect) evidence in favor of these models has been provided by the observation of radio halos with very steep spectra (Brunetti et al. 2008), interpreted as halos in which the radio spectrum starts steepening at frequencies smaller than the observing frequency, thereby favoring poorly efficient acceleration mechanisms.

Acceleration of electrons from the thermal pool to relativistic energies by MHD turbulence in the ICM faces serious energetic problems (e.g. Petrosian & East 2008) and usually leads to large heating of the ICM (Blasi 2000, Petrosian & East 2008). Consequently, turbulent acceleration models start from the assumption of a pre-existing population of relativistic particles that provides the seeds to “reaccelerate” during mergers. The combination of the “unknown” distribution of the seed particles in the ICM with the poorly known properties of turbulence in galaxy clusters reduces the predictive power of this scenario (see however Cassano et al. 2010b and references therein for predictions on the population properties of radio halos). In the context of these models an elegant possibility is based on clusters of galaxies as storage rooms of CRs (Völk et al. 1996, Berezhinsky et al. 1997 and Ensslin et al. 1997) and on the fact that the secondary electrons and positrons produced via inelastic collisions between CR protons and thermal protons in the ICM may be reaccelerated by MHD turbulence during cluster mergers (Brunetti & Blasi 2005, Brunetti & Lazarian 2011). In this sense, this model is of a hybrid nature, but its requirements in terms of CR energy density in clusters are very meek. In this scenario, *off-state* (purely hadronic) radio halos in almost all galaxy clusters should have a radio luminosity  $\sim 10$  times smaller than that of classical *on-state* (turbulent) giant radio halos (Brunetti & Lazarian 2011). The recent detection of diffuse emission in quiescent clusters from stacked analysis of the SUMSS survey may provide the first, possible support for this scenario (Brown et al. 2011).

In these hybrid models  $\gamma$ -rays are produced as a result of the generation and decay of neutral pions and of IC emission from high energy ( $\sim$  TeV) secondary electrons. This realization allows us to gather complementary tests for this scenario based on  $\gamma$ -ray observations. The level of  $\gamma$ -ray emission expected in this scenario is however significantly smaller than that in the pure hadronic case, since the interaction between CR protons and their secondaries with the MHD turbulence enhances the ratio of radio (synchrotron) and  $\gamma$ -ray emission in connection with cluster mergers (Brunetti & Lazarian 2011). Therefore it is easier to achieve consistency between the Fermi-LAT upper limits, radio observations of the spectrum, morphology and Faraday RM (see Brunetti 2011 for a recent review).

In turbulent acceleration models the spectra and morphologies of radio halos depend on the combination of several physical quantities. To provide a simple estimate of the emissivity from a population of reaccelerated electrons we note that the turbulent energy flux that is damped by the coupling with relativistic electrons is eventually converted to synchrotron and IC radiation (Cassano et al. 2007): the bolometric synchrotron emissivity can be written as:

$$J_{syn} \propto \frac{F_{\epsilon_t} \Gamma_{e\pm} / \Gamma_{th}}{1 + (B_{cmb}/B)^2}, \quad (8)$$

where  $F_{\epsilon_t}$  is the energy injection rate of turbulence (per unit volume) and  $\Gamma_{e\pm} / \Gamma_{th} \propto (\epsilon_{e\pm} / \epsilon_{ICM}) \sqrt{T}$  is the ratio of the damping rate of the turbulence by relativistic electrons and by thermal ICM (the second channel of damping goes into thermal heating). If the emitting electrons are secondary particles reaccelerated by the MHD turbulence and assuming that the reacceleration time,  $\tau_{acc}$ , is smaller than the cooling time,  $\tau_{loss}$ , of electrons with energy  $E < E_\nu$  ( $E_\nu$  being the energy of the electrons emitting at the observing frequency), we have  $\epsilon_{e\pm} \propto \epsilon_{CRp} n_{th}$  and Eq. 8 reads :

$$J_{syn}(\nu) \propto n_{th}^{2+f} \frac{B^2}{B^2 + B_{cmb}^2} T^{3/2+f} \Theta(r, \alpha), \quad (9)$$

where we made the simplified assumption  $F_{\epsilon_t} \propto n_{th} T$  (see Cassano et al. 2007 for details).  $\Theta$  is a fudge function to account for several effects. One effect is that in the internal, denser, region of the cluster Coulomb losses can play a role making the reacceleration of secondaries with initial energies  $E \sim 100 - 300$  MeV more difficult. Another effect is that the damping rate of turbulence also depends on the “spectral shape” of relativistic (reaccelerated) particles (Brunetti & Lazarian 2007) that is sensitive to the combination of physical parameters in the ICM. Based on previous calculations (Brunetti & Blasi 2005, Brunetti & Lazarian 2011) we expect that all these effects combine to make the brightness profile flatter.

Eq. 9 essentially implies that the brightness profile from reacceleration of secondary particles is very similar to that based on pure secondary models (with  $\alpha \sim 1$ , Eq. 7), and that two regimes exist (considering  $\Theta \sim$  constant, to evaluate approximate scalings): (i)  $I_{syn} \propto (1+x^2)^{-3\beta(2+f)/2+1/2}$ , for  $B^2(x) \gg B_{cmb}^2$ , and (ii)  $I_{syn} \propto (1+x^2)^{-3\beta(2(1+\eta)+f)/2+1/2}$ , for  $B^2(x) \ll B_{cmb}^2$ .

Predictions from reacceleration of secondary particles differ radically from those of pure hadronic models at high observing frequencies, where  $\tau_{acc} \sim \tau_{loss}$  (or  $\tau_{acc} > \tau_{loss}$ ). Under these conditions the synchrotron spectrum steepens at the frequency (Brunetti et al. 2001):

$$\nu_s \propto \frac{B \tau_{acc}^{-2}}{(B^2 + B_{cmb}^2)^2}, \quad (10)$$

In the IC-dominated regime,  $B < B_{cmb}$ ,  $\nu_s \propto B \tau_{acc}^{-2}$ . Under the simple assumption that the magnetic field strength depends only on distance from the cluster center ( $B(r)$ , *homogeneous models*), the synchrotron spectrum steepens with distance (due to the fact that the emission is produced in a magnetic field that decreases with distance, and assuming an approximately constant acceleration time-scale) and consequently radio halos become smaller at higher observing frequencies. We note indeed that observational claims exist for a decrease of the halo size with frequency and a steepening of the halo spectrum with projected distance (Giovannini et al. 1993, Deiss et al. 1997, see also Fig. 1), although future observations are highly desirable to confirm these findings.

In this section we check that the predictions of the model based on turbulent reacceleration of secondary electrons is consistent with all existing observations and we investigate the implications of the model for the detectability of clusters in  $\gamma$ -rays. The turbulence and particle acceleration process are modelled following Brunetti & Lazarian (2011) <sup>¶¶</sup>, where compressible turbulence is injected at large scales,  $\sim 100$ -300 kpc, and decays onto smaller scales where it behaves as MHD turbulence. The cascading of fast modes is dissipated in the collisionless regime mainly due to transit-time-damping (TTD) with thermal and relativistic particles in the ICM. This process channels a fraction of the turbulent energy flux into the reacceleration of CR protons and secondary electrons. We carry out a homogeneous modeling of turbulence and turbulent reacceleration in the Coma halo, namely we assume a constant ratio  $\epsilon_{tur} / \epsilon_{ICM}$ ,  $\epsilon_{tur}$  being the turbulent energy density, and assume the same scalings between thermal and (the initial) non-thermal properties as in Sect. 2.2. As a reference value we

<sup>¶¶</sup> We refer the readers to Brunetti & Lazarian 2011 for the formalism on turbulence and stochastic particle re-acceleration. It allows us to model self-consistently the effect of turbulent re-acceleration on the spectra of CR protons, secondaries and of the non-thermal emission, going beyond the simplified scalings in Eqs.8-10

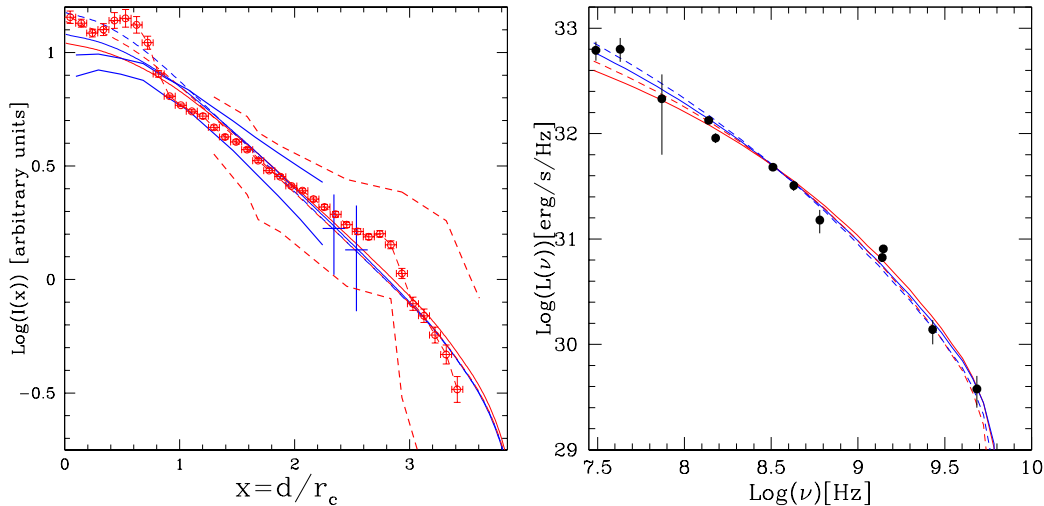


**Figure 5.** **Left:** Brightness (azimuthal averaged) profile of the Coma halo (as in Fig. 1) compared with expectations based on reacceleration models. All models assume  $\epsilon_{tur}/\epsilon_{ICM} \sim 0.05$  on scales  $l < 30$  kpc and  $s=2.6$ . Calculations are carried out assuming (i)  $B_0 = 5\mu\text{G}$  and  $\eta = 0.5$  (solid lines) with  $f = -1.15$  and  $\Delta\tau_r = 0.75$  Gyr (red lines) and  $f = -1.3$  and  $\Delta\tau_r = 0.5$  Gyr (blue lines) ( $\Delta\tau_r$  is the period of reacceleration), and (ii)  $B_0 = 2\mu\text{G}$  and  $\eta = 0.5$  (dashed lines) with  $f = -1.6$  and  $\Delta\tau_r = 0.75$  Gyr (red lines) and  $f = -1.75$  and  $\Delta\tau_r = 0.5$  Gyr (blue lines). **Right:** Spectrum of the Coma halo from reacceleration models as in Left panel. All models are normalised at the radio halo luminosity at 350 MHz.

assume that turbulent motions on scales  $l \leq 30$  kpc contribute to about 5% of the ICM energy (implying a total turbulent budget on the largest scales  $\epsilon_{tur}/\epsilon_{ICM} \sim 0.2$ )<sup>||||</sup>.

In Figure 5 we show the expected brightness profile (left panel) and synchrotron spectrum (right panel) of the Coma halo in the reference case  $\eta = 0.5$  and  $B_0 \sim 5\mu\text{G}$ . The spatial distribution of CR protons must be fairly flat,  $f \sim -1.1$  to  $-1.35$  (up to  $r \sim 3r_c$ ), so as to reproduce the observed radio profile. This is similar to the case of pure hadronic models, although less extreme because in the case of turbulent reacceleration the synchrotron profiles are slightly flatter (a spatially constant distribution of the energy density of CR protons,  $f \sim -1$ , is still consistent with observations) for the reasons discussed above (see Eq. 9 and the paragraph below it). Contrary to the case of pure hadronic models, the steepening of the synchrotron spectrum at higher frequencies is reproduced very well in the case of turbulent reacceleration models allowing a good representation of the data over almost 2 decades in frequency range; more (less) turbulence in the ICM would produce a steepening at higher (lower) frequencies.

During a re-acceleration phase the total energy budget of CR protons within the halo emitting volume ( $r \sim 3r_c$ ) is  $\approx 4\%$  of that of the ICM. This is almost 1 order of magnitude smaller than that in the case of pure hadronic models and implies a smaller  $\gamma$ -ray emission, well consistent with Fermi-LAT limits, as illustrated in Fig. 6.

More  $\gamma$ -rays are produced if the magnetic field in the halo volume is smaller. This allows us to constrain the minimum value of the magnetic field that is required to have a  $\gamma$ -ray flux consistent with Fermi-LAT limits, under the assumption that the halo is generated by reacceleration of secondary particles. In the relevant case  $\eta = 0.5$  we derive a minimum value  $B_0 \geq 2\mu\text{G}$  (Fig. 6) that would imply a magnetic field energy density in the ICM  $\sim 5$  times smaller than the best fit obtained from the analysis of Faraday RM by Bonafede et al.(2010). For the sake of completeness, in Fig. 5 we show the expected synchrotron spectrum and the brightness profile of the Coma halo obtained by assuming  $B_0 = 2\mu\text{G}$  and  $\eta = 0.5$ . In this case the synchrotron emission is always produced under conditions  $B_{IC}^2 \gg B^2$  and a significantly inverted spatial distribution of CR protons,  $f \sim -1.5$  to  $-1.8$  is needed to match the observed brightness profile, with the consequence of a large energy budget in the form of CR protons.

#### 4 DISCUSSION AND CONCLUSIONS

We presented a combined analysis of the spectrum and morphology of the giant radio halo in the Coma cluster, the available measurements of cluster magnetic fields from RM and the upper limits on the  $\gamma$ -ray emission from this cluster as recently

<sup>||||</sup> This reference value is needed to reproduce radio halo properties, see Brunetti & Lazarian 2007, 2011

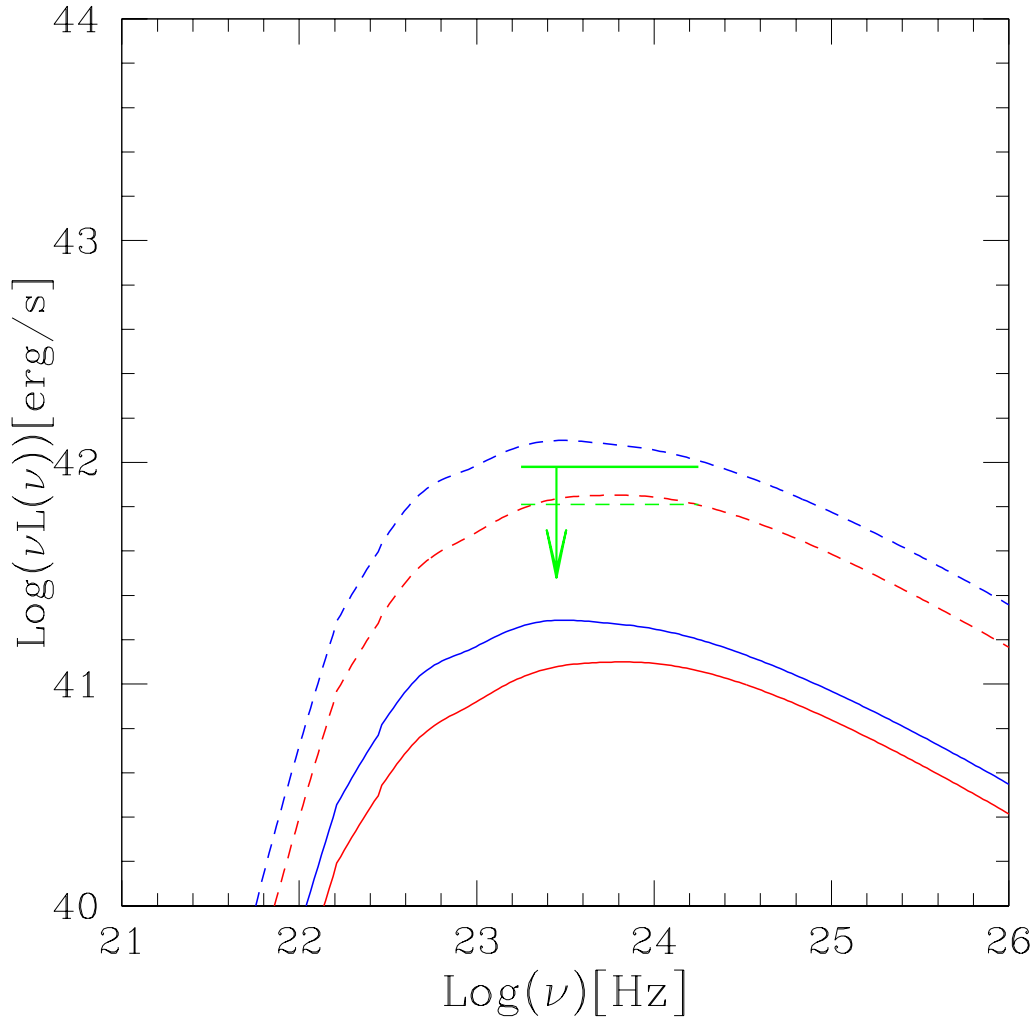


**Figure 6.**  $\gamma$ -ray spectrum due to  $\pi^0$ -decay as expected from reacceleration (hybrid) models. Lines are labelled as in Fig. 5.

obtained by the Fermi-LAT telescope (Ackermann et al. 2010)<sup>\*\*\*</sup>, in the context of models based on secondary electrons: we concentrated on a pure secondary electron model and on a scenario where secondaries are reaccelerated by MHD turbulence during mergers.

#### 4.1 Hadronic models

The pure secondary electron model is based on the concept of CR effective confinement in the ICM (Völk et al. 1996, Berezhinsky et al. 1997) and consists of explaining the giant radio halo emission as the result of synchrotron emission of secondary electrons (and positrons) from inelastic collisions of cosmic ray protons with gas in the ICM. These collisions result in the production and decay of charged and neutral pions. The former lead to production of secondary electrons, while the latter provide a channel of continuous production of gamma radiation. This model has been widely implemented also in cosmological simulations. These simulations, that include, to some extent, CR physics and the acceleration of CRs at cosmological shocks provided a picture of the radio to  $\gamma$ -ray properties of galaxy clusters, under the assumption that the emitting particles (electrons) are generated through pp collisions in the ICM or accelerated at shocks (e.g., Pfrommer et al. 2008 and references therein). The first simulations of this kind predicted that clusters would be potentially detectable in  $\gamma$ -rays with present day  $\gamma$ -ray telescopes (Miniati 2003, Pfrommer 2008). The most important assumption in these simulations is in the efficiency of particle acceleration at weak shocks that is poorly known (see Gabici & Blasi 2003, 2004 and Kang et al. 2007 for a critical view).

<sup>\*\*\*</sup> see also Ando & Nagai (2012) and Han et al. (2012)

More recently, numerical simulations of large-scale structure formation made an attempt to reconcile their results with the lack of detection of galaxy clusters in the  $\gamma$ -ray band (Pinzke & Pfrommer 2010, see also Aleksic et al. 2010,11). Although these simulations provide expectations (still) consistent with the Fermi-LAT upper limits, it is worth mentioning that they do not allow to reproduce the observed properties of radio halos if we assume that halos originate via secondary emission, in particular their (very broad) spatial extent (Donnert et al. 2010a,b; Brown & Rudnick 2011). In this respect, for the sake of completeness, in Fig. 7 we show a comparison between the brightness profile of the Coma radio halo and expectations based on CRs distributions from Pfrommer et al. (2008) and from Pinzke & Pfrommer (2010) simulations. This can be made by using the semi-analytical prescription of the spatial distribution of CR in galaxy clusters, as derived from high resolution numerical simulations of clusters (Pinzke & Pfrommer 2010), and using parameters of the Coma cluster to calculate the production rate of secondaries and the synchrotron emissivity. According to these simulations the ratio of the CR and thermal pressure in typical non-CC clusters is quasi constant up to a distance  $R/R_{vir} \sim 0.2$  and increases by a factor 2-3 up to the virial radius (see Fig.14 in Pinzke & Pfrommer 2010); such an increase is however mainly driven by the temperature decrement in the ICM at large distances.

In reality, the microphysics of the ICM and of CRs in galaxy clusters is very complicated and unfortunately beyond the capabilities of present simulations. For this reason in our paper we have carried out a analysis that does not depend on the way CR protons are generated in the ICM and on the complex processes of CR transport and reacceleration that can take place in the cluster volume. Rather than modeling these complex processes we indeed derived constraints on the spectral and spatial distributions of CR protons directly from the observed spectrum and morphology of the Coma halo, using parameters of the ICM from the X-ray observations (§2.2).

We derived the azimuthally averaged brightness profile of the Coma halo and used it in order to obtain constraints on the spatial profile of the magnetic field strength and of CRs density as functions of the distance from the cluster center. Our profile is obtained using the deep WSRT observations from Brown & Rudnick (2011) and allows us to obtain unprecedented constraints on the non-thermal cluster properties on 3–3.5  $r_c$  scales. We find that fitting the volume averaged radio spectrum of the Coma halo and its azimuthal brightness distribution requires a rather steep spectrum of CR protons,  $s \sim 2.6$ , in the ICM with a spatial distribution much flatter than the spatial distribution of the thermal gas. This leads to an exceedingly large energy content in the form of CRs confined in the ICM and correspondingly large  $\gamma$ -ray emission, exceeding the Fermi-LAT upper limits. Moreover the spectral steepening observed at high frequency can only marginally be explained for the cases with steeper slope ( $s \geq 3$ ) and the combined effect of the SZ decrement. This case is however the one that violates the Fermi-LAT upper limits more clearly.

If we neglect the spectral steepening in our analysis, the model can potentially explain radio observations. However the Fermi-LAT  $\gamma$ -ray limits set a lower limit to the strength of the cluster magnetic field that is in disagreement with a recent analysis of Faraday rotation measures (Bonafede et al. 2010); the more so for steeper spectra of the parent CR protons.

Pure secondary electron models of the Coma halo are thus disfavoured when all available observational data are considered. In this respect any further improvement of upper limits over the next several years, or even a  $\gamma$ -ray detection of the Coma cluster (i.e. with flux 2-3 times smaller the Ackermann et al. limits) will conclusively establish the incompatibility of a hadronic origin of the Coma radio halo with the radio (including RM) and  $\gamma$ -ray observations.

## 4.2 A comment on the most relevant assumptions

A discussion of the assumptions adopted in our analysis is in order. Conclusions derived above are based on canonical assumptions used to model non-thermal emission in galaxy clusters. The most notable assumption is that the CR spectrum in the cluster volume is a power law in momentum,  $N(p) \propto p^{-s}$ , and that the spectrum of secondary particles emitting in the radio band can be calculated under stationary conditions. We constrained the value of the slope  $s$  from the spectrum of the radio halo in the frequency range  $\sim 0.1$ -1 GHz (Fig. 1) and the  $\gamma$ -ray emission of the cluster is calculated by using such values of  $s$ . In principle, the shape of the spectrum of CR protons might also change with location, moving away from cluster core toward the periphery, although there is no strong indication that this may be happening from the total radio spectrum of the Coma halo<sup>\*\*\*</sup>. In this case the expected  $\gamma$ -ray emission is reduced if the spectrum of CR protons is flatter in the regions where the majority of  $\gamma$ -rays are produced, at distances 2–3.5  $r_c$  from the center. This however would result in a halo spectrum that is flatter in the external regions, in contrast with present observations that suggest a “radial spectral steepening” (Giovannini et al 1993, Deiss et al 1997, this is also evident from the comparison between the synchrotron brightness distributions of the halo at 350 and 1400 MHz, Fig. 1).

The situation may change if the spectrum of CRs becomes harder at low enough energies. In this case one may expect that the flux of low energy  $\gamma$ -rays (from decays of neutral pions) is also reduced allowing for some room for pure hadronic models to accommodate current observational constraints. Present radio data limit the possibility of a flattening in the radio spectrum

<sup>\*\*\*</sup> Indeed a mixture of contributions from different power-law spectra results in a “concave” shape of the total synchrotron spectrum.

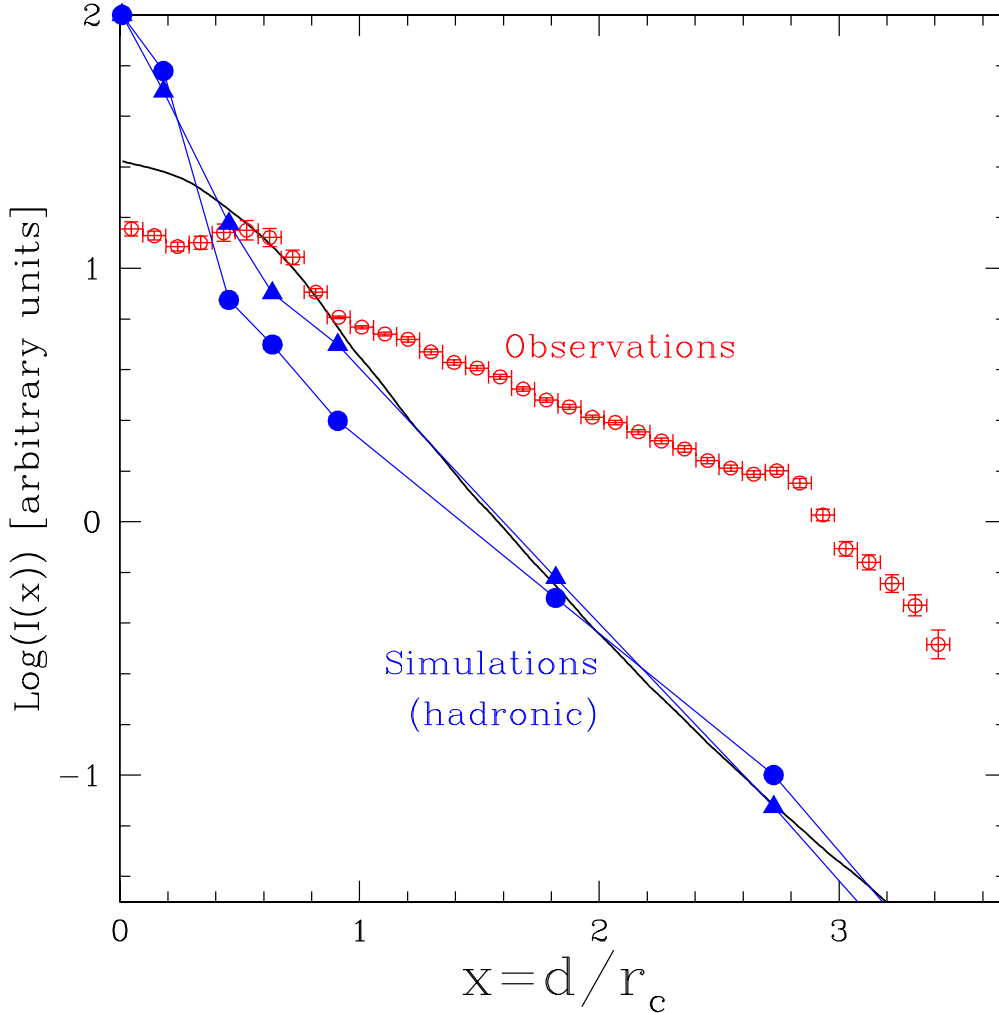


**Figure 7.** Azimuthal averaged brightness profile of the Coma halo (as in Fig. 1) compared with expectations based on numerical simulations that include the acceleration of CR protons and the generation of secondary electrons in the ICM. Points show the expected synchrotron profile from secondary electrons in the massive cluster gs72 from Pfrommer et al. 2008 (circles mark the case of radiative simulations). The solid line (black) show the expectations based on the semi-analytic model of CR protons in Coma based on numerical simulations (Pinzke & Pfrommer 2010). A magnetic field profile  $B(r)^2 \propto \epsilon_{ICM}$  and  $B_0 = 5\mu\text{G}$  are assumed.

to frequencies  $\nu \leq 100$  MHz, leading to a limit to the energy where a possible break occurs in the spectrum of the primary CR protons,  $E_b \leq 10 - 20$  GeV. Under these conditions we note that a substantial reduction of the  $\gamma$ -ray luminosity due to  $\pi^0$ -decay in the 1-10 GeV band, necessary to make hadronic models still consistent with –at least– the limits derived from the first 18 month of FERMI-LAT data (Ackermann et al. 2010) (Fig. 2), would require a prominent CR spectral break, by  $\Delta s \geq 0.5$ .

The two points that disfavour pure hadronic models for the radio halo are the steepening of the halo spectrum observed at higher frequencies and the inconsistency between the properties of the cluster magnetic field constrained by Faraday RM and by Fermi-LAT limits under the assumption of a hadronic origin of the halo. The latter point however might simply indicate that RM and synchrotron emission trace different magnetic fields. As already mentioned in Sect. 2.3 the simplest way to have RM and synchrotron emission sample different fields is to assume that some of the RM come from regions adjacent to and influenced by the radio sources, in this case however the magnetic field in the ICM as inferred from the analysis of RM would likely be biased to higher values of the magnetic field (Rudnick & Blundell 2003) thus making the inconsistency between magnetic fields even stronger. On the other hand, if one assumes that RM originates entirely in the ICM, RM and synchrotron emission may sample different fields in the case of a highly inhomogeneous fields, because the synchrotron emissivity depends non-linearly on the magnetic field and its fluctuations. Positive fluctuations however increase also the radiative losses of

particles (assuming they vary on time scale sufficiently long,  $> 10^7 - 10^8 \text{ yrs}^{***}$ ) and this is expected to partially quench the expected boosting of the synchrotron emissivity of electrons generated in regions with medium/high fields. Under (at least quasi-) stationary conditions the emissivity reads:

$$\langle J_{syn} \rangle_{Volume} = \alpha \hat{B}^{1+\alpha} \frac{(1 + (\delta B / \hat{B})^2)^{(1+\alpha)/2}}{\hat{B}^2 + \delta B^2 + B_{cmb}^2}, \quad (11)$$

where we introduced a magnetic field made of a large scale component  $\hat{B}$  and a turbulent component  $\delta B$ , such that  $\langle \hat{B} + \delta B \rangle_{Volume} = \hat{B}$  and  $\langle \hat{B} + \delta B \rangle_{Volume}^2 = \hat{B}^2 + \delta B^2$ . Under these assumptions we estimate that the ratio of  $\gamma$ -ray and radio cluster luminosities decreases by (only) a factor  $\sim 1.7$ , compared to results using the formalism in Sect. 2.1, if we assume  $\delta B^2 \sim \hat{B}^2$ , with  $\delta B^2$  anchored to the best fit value from RM studies (normalisation and spatial profile).

On the other hand, RMs suggest that  $\delta B \gg B$ , in which case Eq.11 becomes equivalent to Eq.4 in Sect. 2.1\*\*\*. In this sense the question of whether Faraday RM and synchrotron emission measure the same magnetic field only lies in the capability of RM studies to provide a good description of the ICM magnetic field. Future radio telescopes, including LOFAR and SKA, will greatly improve the sensitivity to RMs allowing to detect and use many tens of background radio sources per clusters to sample magnetic fields along many lines of sight, thus removing potential biases in present studies.

Finally, for the sake of completeness we mention that in principle, spatial diffusion of particles in inhomogeneous fields may also affect the value of the ratio synchrotron/ $\gamma$ -ray luminosity in hadronic models, if the diffusion time necessary to cover the spatial scales on which field inhomogeneities occur is smaller than both the life-time of particles and the time-scale of magnetic field (local) variations. This however depends on the details of the magnetic field and diffusion model.

### 4.3 Beyond the pure hadronic model: turbulent reacceleration of secondaries

In §3 we went beyond the pure hadronic model and discussed the case of the reacceleration model were secondary particles are reaccelerated by MHD turbulence. We find that this model allows to obtain a good description of the radio spectrum and morphology of the Coma cluster and at the same time they may easily be compatible with the Fermi-LAT upper limits on the  $\gamma$ -ray emission from this cluster and with the measured magnetic field strength as inferred from RMs.

In the simplified assumption that both the ratios of turbulent and thermal energy density,  $\epsilon_{tur}/\epsilon_{ICM}$ , and of magnetic field and thermal energy density,  $\epsilon_B/\epsilon_{ICM}$ , are constant in the radio emitting volume, the brightness profile of the Coma halo leads us to infer that the spatial distribution of CRs in the cluster should be very broad, flat (or slightly increasing in the external regions) on the halo size-scale. This is because the particular reacceleration model adopted in this paper faces drawbacks that are in part similar to those of a pure hadronic model for the origin of the halo. This is simply because the seed electrons for reacceleration are generated by proton-proton collisions in the ICM. A flat spatial distribution of CRs is a fairly strong requirement, although possible support for a rather flat distribution of CRs, significantly broader than that of the thermal ICM, comes from very recent numerical cosmological simulations that include CRs accelerated at shocks (Vazza et al. 2012). Present radio data do not constrain the energy density of CR protons on scales larger than the halo size-scale. However if we speculate that the flat spatial distribution of CR protons extends on larger scales the resulting energy budget of CRs in the cluster would be significantly larger than that required by our modeling.

In general several, effects may contribute to mitigate this situation. First, numerical simulations show that the turbulent energy density (and the ratio  $\epsilon_{tur}/\epsilon_{ICM}$ ) increases outside the cores of simulated clusters (Vazza et al. 2009, 11; Iapichino & Niemeyer 2008, Iapichino et al. 2011), implying a synchrotron brightness profile potentially flatter than that calculated under the assumption of a constant ratio  $\epsilon_{tur}/\epsilon_{ICM}$ . Second, we limit our analysis to the case  $B^2 \propto \epsilon_{ICM}$  ( $\eta = 0.5$ ), that gives the best fit to Faraday RM. On the other hand for smaller values of  $\eta$  the spatial distribution of CR protons that is required by the model to match the observed synchrotron brightness profile of the halo is significantly steeper with radius, although still flatter than the distribution of the thermal energy density of the cluster. Finally we note that the situation is greatly mitigated as soon as one would relax the assumption of having only secondary electrons in the ICM. Indeed primary electrons accelerated at shocks, or during the activity of cluster galaxies and AGN, can survive a substantial fraction of the Hubble time in the cluster outskirts (e.g. Sarazin 1999). These primaries provide a natural population of seed electrons to reaccelerate in a turbulent ICM (Brunetti et al 2001, Petrosian 2001) and may significantly contribute to the synchrotron emission in the external regions of giant radio halos. If a substantial contribution to the radio halo emission comes from the reacceleration of primary electrons, the expected  $\gamma$ -ray emission from the Coma cluster becomes even smaller than that calculated in §3.

\*\*\* The minimum RM scale of about 2 kpc for Coma radio galaxies derived by Bonafede et al 2010, and the typical fractional polarization of about 10%, imply that any ICM fluctuation on smaller scales, that could be very intermittent, must be weak.

\*\*\* In the analysis by Bonafede et al. the magnetic field is parameterised with a power spectrum  $B^2 = 8\pi \int P_B(k) dk$  between a maximum and minimum scale and its properties are constrained by comparing observations with simulated Faraday Rotation maps derived for different parameters

Ongoing and future observations in the deep non-thermal (high and very-high energy) regime of the Coma cluster will therefore provide precious information on its non-thermal content.

## ACKNOWLEDGEMENTS

Authors acknowledge useful comments from the anonymous referee and discussions with J. Donnert and T. Jeltema. GB acknowledges partial supported by INAF under grant PRIN-INAF 2009. LR acknowledges support, in part, by U.S. National Science Foundation grant AST-0908688 to the University of Minnesota. AB acknowledges partial supported by the DFG Research Unit 1254 “Magnetization of interstellar and intergalactic media: the prospect of low frequency radio observations”.

## REFERENCES

- Ackermann M., et al. 2010, ApJ 717, L71  
 Ando, S., & Nagai, D. 2012, arXiv:1201.0753  
 Aleksic J., et al. 2010, ApJ 710, 634  
 Aleksić, J., Alvarez, E. A., et al. 2011, arXiv:1111.5544  
 Aharonian F.A., et al., 2009a, A&A 495, 27  
 Aharonian F.A., et al., 2009b, A&A 502, 437  
 Berezhinsky V.S., Blasi P., Ptuskin V.S., 1997, ApJ 487, 529  
 Blasi, P. 2000, ApJ, 532, L9  
 Blasi P., 2001, APh 15, 223  
 Blasi P., Colafrancesco S., 1999, APh 12, 169  
 Blasi P., Gabici S., Brunetti G., 2007, IJMPA 22, 681  
 Bonafede A., Feretti L., Murgia M., Govoni F., Giovannini G., Dallacasa D., Dolag K., Taylor G.B., 2010, A&A 513, 30  
 Bonafede, A., Govoni, F., Feretti, L., et al. 2011a, A&A, 530, A24  
 Bonafede A., Dolag K., Staszyn F., Murante G., Borgani S., 2011b, MNRAS 418, 2234  
 Briel U.G., Henry J.P., Böhringer H., 1992, A&A 259, L31  
 Brown S., Rudnick L., 2011, MNRAS, 412, 2  
 Brown, S., Emerick, A., Rudnick, L., & Brunetti, G. 2011, ApJ, 740, L28  
 Brunetti, G. 2004, JKAS, 37, 493  
 Brunetti G., 2009, A&A 508, 599  
 Brunetti, G. 2011, MmSAI, 82, 515  
 Brunetti G., Setti G., Feretti L., Giovannini G., 2001, MNRAS 320, 365  
 Brunetti G., Blasi P., 2005, MNRAS 363, 1173  
 Brunetti G., Lazarian A., 2007, MNRAS, 378, 245  
 Brunetti, G., Venturi, T., Dallacasa, D., et al. 2007, ApJ, 670, L5  
 Brunetti G., Giacintucci S., Cassano R., Lane W., Dallacasa D., Venturi T., Kassim N.E., Setti G., Cotton W.D., Markevitch M., 2008, Nature 455, 944  
 Brunetti G., Cassano R., Dolag K., Setti G., 2009, A&A 507, 661  
 Brunetti G., Lazarian A., 2011, MNRAS, 410, 127  
 Cassano R., Brunetti G., 2005, MNRAS 357, 1313  
 Cassano, R., Brunetti, G., Setti, G., Govoni, F., & Dolag, K. 2007, MNRAS, 378, 1565  
 Cassano, R., et al., 2008, A&A, 480, 687  
 Cassano R., Etori S., Giacintucci S., Brunetti G., Markevitch M., Venturi T., Gitti M., 2010a, ApJ 721, L82  
 Cassano, R., et al., 2010b, A&A, 509, 68  
 Churazov E., Vikhlinin A., Zhuravleva I., et al., 2012, MNRAS 421, 1123  
 Colafrancesco, S., & Blasi, P. 1998, Astroparticle Physics, 9, 227  
 Colafrancesco, S., Marchegiani, P., Perola, C., 2005, A&A 443, 1  
 Dallacasa D., et al., 2009, ApJ, 699, 1288  
 Deiss, B. M., Reich, W., Lesch, H., & Wielebinski, R. 1997, A&A, 321, 55  
 Dennison B., 1980, ApJ, 239, L93  
 Dermer C.D., 1986a, ApJ 307, 47  
 Dermer C.D., 1986b, A&A 157, 223  
 Dolag K., Ensslin T.A., 2000, A&A 362, 151  
 Donnert J., Dolag K., Brunetti G., Cassano R., Bonafede A., 2010a, MNRAS 401, 47  
 Donnert J., Dolag K., Cassano R., Brunetti G., 2010b, MNRAS 407, 1565  
 Enßlin, T. A. 2002, A&A, 396, L17  
 Enßlin, T. A., Biermann, P. L., Kronberg, P. P., & Wu, X.-P. 1997, ApJ, 477, 560  
 Enßlin, T., Pfrommer, C., Miniati, F., & Subramanian, K. 2011, A&A, 527, A99  
 Feretti, L., Fusco-Femiano, R., Giovannini, G., & Govoni, F. 2001, A&A, 373, 106  
 Ferrari, C.; Govoni, F.; Schindler, S.; Bykov, A. M.; Rephaeli, Y., 2008, SSRv 134, 93  
 Fujita Y., Takizawa M., Sarazin C.L., 2003, ApJ 584, 190  
 Gabici S., Blasi P., 2003, ApJ 583, 695  
 Gabici, S., & Blasi, P. 2004, Astroparticle Physics, 20, 579

- Giovannini G., Feretti L., Venturi T., Kim K.-T., Kronberg P.P., 1993, ApJ 406, 399
- Giovannini, G., Tordi, M., Feretti, L., 1999, NewA, 4, 141
- Giovannini, G., et al., 2009, A&A, 507, 1257
- Govoni F., Ensslin T.A., Feretti L., Giovannini G., 2001, A&A 369, 441
- Guidetti, D., Laing, R. A., Bridle, A. H., Parma, P., & Gregorini, L. 2011, MNRAS, 413, 2525
- Han, J., Frenk, C. S., Eke, V. R., Gao, L., & White, S. D. M. 2012, arXiv:1201.1003
- Jeltema T.E., Profumo S., 2011, ApJ, 728, 53
- Kang, H., Ryu, D., Cen, R., & Ostriker, J. P. 2007, ApJ, 669, 729
- Kempner, J. C., Sarazin, C. L., 2001, ApJ, 548, 639
- Keshet U., 2010, arXiv:1011.0729
- Keshet U., Loeb A., 2010, ApJ, 722, 737
- Kushnir, D., Katz, B., & Waxman, E. 2009, JCAP, 9, 24
- Iapichino, L., Niemeyer, J. C., 2008, MNRAS, 388, 1089
- Iapichino, L., Schmidt, W., Niemeyer, J. C., & Merklein, J. 2011, MNRAS, 414, 2297
- Macario G., Venturi T., Brunetti G., Dallacasa D., Giacintucci S., Cassano R., Bardelli S., Athreya R., 2010, A&A, 517, 43
- Marchegiani P., Perola G. C., Colafrancesco S., 2007, A&A 465, 41
- Miniati, F. 2003, MNRAS, 342, 1009
- Moskalenko I.V., Strong A.W., 1998, ApJ 493, 694
- Murgia, M., et al., 2009, A&A, 499, 679
- Perkins, J. S., Badran, H. M., Blaylock, G., et al. 2006, ApJ, 644, 148
- Petrosian V., 2001, ApJ 557, 560
- Petrosian V., East W.E., 2008, ApJ 682, 175
- Pfrommer C., 2008, MNRAS 385, 1242
- Pfrommer C., Ensslin T.A., 2004, MNRAS 352, 76
- Pfrommer C., Ensslin T.A., Springel V., 2008, MNRAS 385, 1211
- Pinzke, A., & Pfrommer, C. 2010, MNRAS, 409, 449
- Pizzo, R., 2010, *Tomography of galaxy clusters through low-frequency radio polarimetry*, PhD Thesis, Groningen University
- Reimer A., Reimer O., Schlickeiser R., Iyudin A., 2004, A&A 424, 773
- Reimer O., Pohl M., Sreekumar P., Mattox J.R., 2003, ApJ 588, 155
- Ribicky G.B., Lightman A.P., *Radiative Processes in Astrophysics*, New York, Wiley-Interscience, 1979
- Rudnick, L., & Blundell, K. M. 2003, ApJ, 588, 143
- Sarazin, C.L. 1999, ApJ 520, 529
- Sarazin, C. L. 2004, JKAP, 37, 433
- Schlickeiser R., Sievers A., Thiemann H.: 1987, A&A 182, 21
- Thierbach M., Klein U., Wielebinski R., 2003, A&A 397, 53
- van Weeren, R. J., Brügger, M., Röttgering, H. J. A., et al. 2011, A&A, 533, A35
- Vazza, F., Brunetti, G., Kritsuk, A., et al. 2009, A&A, 504, 33
- Vazza, F., et al., 2011, A&A, 529, 17
- Vazza, F., Brügger, M., Gheller, C., & Brunetti, G. 2012, arXiv:1201.3362
- Venturi, T. 2011, MmSAI, 82, 499
- Völk H.J., Aharonian F.A., Breitschwerdt D., 1996, SSRv 75, 279
- Völk, H. J., & Atoyan, A. M. 1999, *Astroparticle Physics*, 11, 73
- Willson, M. A. G., 1970, MNRAS, 151, 1
- Wolfe, B., Melia, F., Crocker, R. M., & Volkas, R. R. 2008, ApJ, 687, 193